Journal of Catalysis **209,** 177–185 (2002)
doi:10.1006/jcat.2002.3598

Simultaneous Determination of Reaction Kinetics and Oxygen Activity in Single-Phase Oxidic Catalysts and Their Mixture during Partial Oxidations

M. Estenfelder[1] and H.-G. Lintz[2]

Institut für Chemische Verfahrenstechnik, Universität Karlsruhe (TH), 76128 Karlsruhe, Germany

Received December 13, 2001; revised February 19, 2002; accepted February 25, 2002

The partial oxidation of an aldehyde to a carboxylic acid has been studied over two single-phase oxidic catalysts and a mixture of both phases. One phase was mainly based on Mo and V (Mo–V–O_x); the other was a copper molybdate, $CuMoO_4$. The experimental setup enabled the simultaneous determination of reaction kinetics and the oxygen activity of the catalyst under working conditions. The kinetic measurements were performed by monitoring the gas-phase composition along the length of a fixed bed of catalyst which was loaded into a sample port reactor. The reactor was treated as an isothermal plug-flow system. Over Mo–V–O_x the aldehyde could be oxidised to the corresponding acid with high activity and selectivity (maximum acid yield: 92 mol%). In contrast, the copper molybdate proved to be nearly inactive and unselective with respect to the acid production under the same reaction conditions, with the maximum yield of the acid always being below 2 mol%. Surprisingly, the selectivity towards the acid and as a consequence the acid yield could be significantly improved (maximum acid yield: 95 mol%) by mechanically mixing both oxidic phases. This demonstrates a synergism between the Mo–V–O_x and the copper molybdate in the case of the partial oxidation investigated. The simultaneous determination of the oxygen activity in the catalyst has been realised by use of a solid electrolyte potentiometry (SEP) cell, connected to the apparatus. The cell consists of an oxygen ion-conducting solid electrolyte ($ZrO_2 + 8.5$ wt% Y_2O_3) coated with a platinum reference electrode on one side and with the catalytically active electrode on the other side. While the measuring electrode was in contact with the gas phase to be analysed, the reference electrode was always flushed with air. We used the same catalyst in the tubular reactor (typical acrylic acid catalyst Mo–V–Cu–O_x) for all potentiometric measurements in order to obtain the same gas-phase composition over the measuring electrode. The oxygen activity of the catalyst is derived from the measured potential difference between both electrodes. The results of the potentiometric measurements show that both single-phase catalysts, the Mo–V–O_x and the copper molybdate, are always in a reduced state under working conditions. As long as a significant amount of the aldehyde (>0.2 mol%) was present in the gas phase the Mo–V–O_x remained in a highly reduced state, reflecting the strong interaction between the aldehyde and the Mo–V–O_x. The less reduced state of Mo–V–O_x in contact with a mixture containing the carboxylic acid instead of the aldehyde reflects the weaker interaction of Mo–V–O_x with the intermediate carboxylic acid. In contrast, the reduction of the copper molybdate catalyst was more pronounced in contact with a mixture containing the acid instead of the aldehyde. This indicates that the rate of the total oxidation of the acid is higher than the rate of its formation, which is the main reason for the low acid yields over the copper molybdate. The oxygen activity in Mo–V–Cu–O_x (1), which can be regarded as a mixture of Mo–V–O_x and $CuMoO_4$, lay between the values for the single oxides, which can be interpreted by the transport of oxygen from the donor-phase $CuMoO_4$ to the acceptor-phase Mo–V–O_x. The transferred oxygen may act as a selective species, thus increasing the selectivity of the aldehyde oxidation with respect to the corresponding acid.

Key Words: synergism; donor; acceptor; solid electrolyte potentiometry; oxygen activity; oxidation reaction; oxygen transfer; kinetic, *in situ*.

1. INTRODUCTION

Multicomponent oxidic catalysts are commonly used in the partial oxidation of hydrocarbons and other organic compounds. They may show (2)—at reasonably high activities—extremely good selectivities for the products aimed at. The efficiency of such catalysts and the synergy effects observed in the presence of one or more well-defined oxidic phases raise the question of their origin. Different explanations for these synergetic effects, i.e., the enhancement of both activity and selectivity, have been proposed (3). According to the concept of "site isolation" (4) high selectivities to the partially oxidised intermediate can be obtained if the amount of oxygen at an active site of a catalyst is limited to such an extent that the total oxidation reaction, which requires more oxygen than the partial oxidation reaction, cannot occur for stoichiometric reasons. This might be realised by properly adjusting the degree of reduction of the catalyst or partly covering the active phase with another one. In the "oxygen transfer" concept it is assumed

[1] Current address: Consortium für elektrochemische Industrie GmbH, Zielstattstraße 20, 81379 München, Germany.

[2] To whom correspondence should be addressed. Fax: +49-(0)721-608-6118. E-mail: Cvt@ciw.uni-karlsruhe.de.

0021-9517/02 $35.00

that mobile oxygen species which are transferred from the so-called oxygen donor phase to the acceptor phase might dramatically influence the catalytic behaviour of the latter phase. Concerning the mechanism of oxygen transfer in the solid and the function of the transferred oxygen species different explanations are given. According to the "remote control" theory developed by Delmon and Weng (5) the mobile oxygen species are transferred via surface migration ("spillover") from the so-called donor phase to the acceptor phase. Teichner (6) defines spillover as the "mobility of sorbed species from one phase on which it is easily adsorbed onto another phase where it does not directly adsorb." Although the spillover oxygen species might also act as a true reactant its main role in the remote-control concept is the creation or regeneration of active sites on the acceptor phase, for example by efficiently eliminating coke (5). In contrast to the remote-control concept Moro-Oka (7) claims that in the case of propene oxidation over the oxidic mixture Bi–Mo–O_x/Co–Fe–Mo–O_y oxygen is transferred from Co–Fe–Mo–O_y via bulk migration through lattice vacancies (O^{2-}) to the Bi–Mo–O_x, on the surface of which the oxidation of propene occurs. Thus Moro-Oka states that oxygen is transferred through the bulk as an ionic species and furthermore is directly involved in the partial oxidation reaction. Ozkan *et al.* (8) explain the observed phase synergism between $MnMoO_4$ and MoO_3 during oxidation of butene, butadiene, and furane similarly. They state that oxygen species are transferred from $MnMoO_4$ to MoO_3 to reoxidise the reduced active sites of MoO_3, where the transformation of butene occurs. Due to the special role of each phase—one phase incorporating gas-phase oxygen in the lattice, the other phase transferring lattice oxygen in the adsorbed reactant molecule—Ozkan speaks of "job distribution."

Besides the different concepts for explaining the synergy in mixed oxides it is pointed out in the literature that the nature of the oxygen species, which is transferred from the catalyst to the adsorbed reactant to be oxidised, might determine whether the desired partial oxidation reaction or the total oxidation takes place. Most authors agree that usually only the participation of nucleophilic lattice oxygen species (O^{2-}) leads to partial oxidation whereas adsorbed oxygen species (O_2) and electrophilic species (O, O^-, O_2^-) favour total oxidation (3). This concept—the participation of lattice oxygen in the selective oxidation reaction—is widely accepted in the literature and is claimed, for example, for the oxidation of isobutyric acid over heteropolyacids (9) and for the oxidation of acrolein to acrylic acid over Mo–V–oxides (10).

Anyhow, the availability and transfer of oxygen is a function of the phase composition of the catalyst, i.e., its oxidation state. Under operating conditions the oxidation state results from the rates of oxygen transfer to and from the solid. There is a mutual interaction of the gas phase and the catalysing solid. To characterise the oxidation state of a solid, Wagner (11) proposed the measurement of its oxygen activity by a potentiometric method. It is based on the use of an ion-conducting solid as electrolyte. Two porous electrodes of a galvanic cell are separated, gas tight, by the solid electrolyte. One electrode is exposed to the reacting gas mixture and acts simultaneously as the catalyst; the second electrode is in contact with a given value of the oxygen partial pressure as reference. The measurement of the potential difference between these two electrodes leads to the value of the oxygen activity in the catalyst, which is operationally defined by this method, named solid electrolyte potentiometry (SEP).

In the following we present an experimental setup which allows the simultaneous determination of the gas-phase composition and the oxygen activity of the solid catalyst under operating conditions along a tubular fixed-bed reactor. Furthermore, we show that in the case of acrolein oxidation over an oxidic multicomponent catalyst, mainly consisting of Mo, V, and Cu, a significant synergistic effect with respect to the selectivity of acrylic acid formation exists. The *in situ* determination of the oxygen activity of the single phases and a mixture of both phases gives us a hint as to the nature of the observed synergism.

2. METHODS

The experimental setup (cf. Fig. 1) has already been described in (12). It can be divided into two parts: the fixed-bed reactor used for the kinetic measurements, and a second device intended for the solid electrolyte potentiometry.

2.1. Kinetic Measurements

The reaction mixture is admitted through thermal mass flow controllers, with the concentrations of acrolein and water being fixed by loading a stream of nitrogen or air via two saturation–condensation systems operated at constant

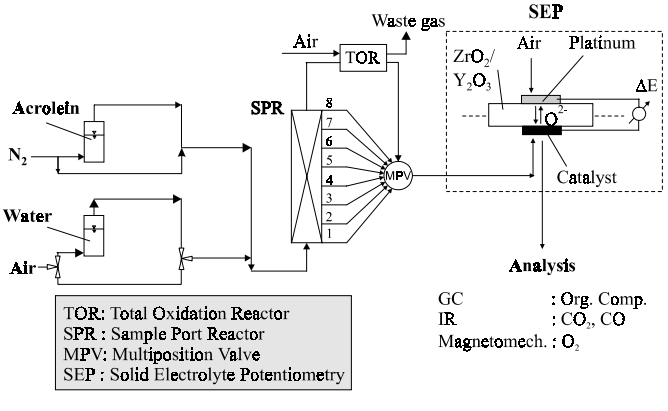

FIG. 1. Schematic diagram of the experimental setup.

pressure and temperature. The kinetic experiments were carried out in a tubular reactor (1500-mm length, 15-mm internal diameter) under isothermal conditions at a pressure of 1.4 bar and at temperatures of 533 and 573 K. A fixed bed consisting of about 200 g of spherical eggshell catalyst was employed. The feed stream contained 4 mol% acrolein, 3–11 mol% oxygen, 5 mol% water, and balance nitrogen at volume flow rates of 60 or 80 ml/s (NTP).

The reactor was divided into seven segments with separate electrical heating to maintain isothermal conditions. At the end of each segment a small side stream was withdrawn by use of heated capillaries. Each side stream selected by use of a multiposition valve entered the solid electrolyte potentiometry (SEP) cell (cf. Section 2.2) and was subsequently analysed by gas chromatography (organic components), infrared photometers (CO, CO_2), and a magnetomechanic device (O_2).

2.2. Potentiometric Measurements

Each side stream collected at the sample ports sequentially passed over the catalyst electrode of the SEP cell shown in Fig. 1.

SEP was carried out in a galvanic cell consisting of a solid electrolyte disk (thickness, 2 mm) made of yttria (8.5 wt%)-stabilised zirconia, coated with the oxidic catalyst on the measuring side, and with a porous platinum electrode on the reference side. The measuring electrode was in contact with the gas phase to be analysed and simultaneously worked as a catalyst. The catalyst electrode has been prepared in a way that acrolein conversion in the cell was kept below 10% in any case. Thus, we can safely assume a constant gas-phase composition over the catalyst electrode. In addition, there were no inner transport resistances due to the small film thickness (<50 μm) of the catalyst electrode. The reference electrode was flushed with air. Both electrodes were connected via a high-ohmic volt meter. The measured potential difference between both electrodes is characteristic of the oxidation state of the catalyst electrode under working conditions. The pressure in the cell was the same as in the fixed-bed reactor ($p = 1.4$ bar); the temperature was adjusted to 573 K in all cases.

During the potentiometric measurements the operating conditions in the tubular reactor, containing the typical acrylic acid catalyst Mo–V–Cu–O_x (1), were kept constant. Therefore, the axial concentration profiles remained the same and we measured the response of different oxidic electrodes to an identical profile in the gas phase.

2.3. Catalyst Preparation for the Fixed Bed

The fixed bed contained 200 g of a spherical eggshell catalyst, diluted by shattered steatite particles (0.9 mm < d < 1.6 mm) in a mass ratio of 1 : 1 to ascertain plug-flow conditions. The eggshell catalysts used throughout the study were prepared by coating spherical steatite particles of 4- to 5-mm diameter with a porous oxidic layer. The final catalysts employed during the kinetic measurements contained 10 or 20 wt% active mass corresponding to a shell thickness of 100 and 220 μm.

TABLE 1

Preparation of EggShell Catalysts Used for the Kinetic Measurements in the Fixed-Bed Reactor

Catalyst	Active mass (wt%)	Shell thickness (μm)	Preparation
$CuMoO_4$	10	100	Single phase (13)
Mo–V–O_x	20	220	Single phase (14)
Mo–V–O_x/$CuMoO_4$	20	220	Mechanical mixture of single oxides
Mo–V–Cu–O_x (typical acrylic acid catalyst)	10	100	Mixed oxides
	20	220	one-pot synthesis (1)

The pure oxidic phases, $CuMoO_4$ and Mo–V–O_x, used throughout the kinetic measurements have been described in detail elsewhere (13, 14). The mechanical mixture of both phases was obtained by mixing the powder of the pure phases at a mass ratio $m_{CuMoO_4}/m_{Mo\text{–}V\text{–}O_x}$ of 1/8. The typical acrylic acid catalyst mainly contains Mo, V, and Cu and is prepared in a so-called one-pot synthesis according to (1). For the mentioned reason we used the same fixed-bed catalyst in the tubular reactor—the typical acrylic acid catalyst with 10 wt% active mass—in all potentiometric measurements. The different catalysts used are summarised in Table 1.

2.4. Electrode Preparation

The reference electrode was prepared by coating the electrolyte with a thin layer (80 μm) of a commercial platinum paste and sintering the film for 2 h at a temperature of 800°C. The measuring electrodes consisted of the same catalyst powder (1, 13, 14) which was used to prepare the eggshell catalysts. Each catalyst powder was mixed with an organic binder, giving a viscous paste. The solid electrolyte was coated with this paste up to a film thickness of 50 μm and sintered for 1 h at 320°C, leading to a sufficient adherence of the porous electrode on the electrolyte. Details are reported in (15).

2.5. Data Evaluation

2.5.1. Kinetic measurements. By using the experimental setup shown in Fig. 1 we measured concentration profiles as a function of the modified residence time t_m, which is defined by the ratio of the mass of the catalytically active oxide $m_{C,z}$ between reactor inlet and sample port z and the volumetric flow rate $\dot{V}$ through the reactor:

$$t_{m,z} = \frac{m_{C,z}}{\dot{V}}. \qquad [1]$$

Because of the constant volumetric flow rate throughout the reactor we can define the acrolein conversion X_z up to sampling port z,

$$X_z = \frac{c_{\text{Acrolein, in}} - c_{\text{Acrolein},z}}{c_{\text{Acrolein, in}}}, \qquad [2]$$

and the integral reactor selectivity ${}^{\text{R}}S_{i,z}$ for the formation of product i measured at port z,

$${}^{\text{R}}S_{i,z} = \frac{c_{i,z} \cdot \varepsilon_i}{(c_{\text{Acrolein, in}} - c_{\text{Acrolein},z}) \cdot \varepsilon_{\text{Acrolein}}}. \qquad [3]$$

By using the dimensionless factor ε_i, which designates the number of carbon atoms in one molecule of species i, the reactor selectivity is normalised to values between zero and one.

It has been shown earlier that the kinetics of selective acrolein oxidation over oxidic catalysts can be described by using a simple network (cf. Fig. 2) of chemical reactions (15, 16). CO_2, CO, and acetic acid generated in small amounts can be lumped together into one pseudospecies ("by-products").

The network consists of the main reaction from acrolein to acrylic acid, a parallel reaction of acrolein to by-products, and the consecutive reaction of acrylic acid to by-products.

The rate of the individual reactions in this system can be represented by the rate equations listed below, where the reaction rate $r_{\text{m}i,j}$ in pathway i, j is given in moles per gram per second. All rate coefficients $k_{\text{m}i,j}$ are related to the mass of the catalytically active compound. Mass balancing the reactor in steady state leads to a set of three differential equations which can be solved numerically by use of the Runge–Kutta method. The values of the kinetic coefficients $k_{\text{m}i,j}$ and b are determined by curve fitting of the calculated concentration profiles to the experimentally determined ones.

We can derive characteristic parameters for the activity and selectivity of the used catalyst from these coefficients:

- Due to the fractional order of the parallel reactions $r_{\text{m}1,2}$ and $r_{\text{m}1,3}$ we make use of a conversion-dependent parameter $k^*_{\text{m}1}$ characterising the activity of the catalyst with respect to acrolein conversion:

$$k^*_{\text{m}1} = \frac{k_{\text{m}1,2} + k_{\text{m}1,3}}{1 - \frac{b \cdot X^*}{\ln(1 - X^*)}} = k^*_{\text{m}1,2} + k^*_{\text{m}1,3}. \qquad [7]$$

$k^*_{\text{m}1}$ may be considered the pseudo first-order rate coefficient giving the same acrolein conversion X^* at the same residence time t_{m} at the reactor outlet. Its derivation has been described elsewhere (15, 17). $k^*_{\text{m}1}$ is calculated for $X^* = 0.99$, as the maximum yield of acrylic acid was always obtained at conversions near that value except in the case of $CuMoO_4$.

- For a given catalyst and temperature the course of the selectivity with respect to the production of the intermediate acrylic acid as a function of conversion is fixed by two parameters, the grain selectivity towards acrylic acid ${}^{\text{K}}S_{\text{Acrylic Acid}}$,

$${}^{\text{K}}S_{\text{Acrylic Acid}} \equiv \lim_{X_{\text{Acrolein}} \to 0} {}^{\text{R}}S_{\text{Acrylic Acid}} = \frac{k_{\text{m}1,2}}{k_{\text{m}1,2} + k_{\text{m}1,3}}, \qquad [8]$$

and the integral stability of the metastable intermediate acrylic acid,

$${}^{\text{int}}\lambda_{\text{Acrylic Acid}} = \frac{k^*_{\text{m}1,2}}{k_{\text{m}2,3}}, \qquad [9]$$

with $k^*_{\text{m}1,2}$ designating an integral rate constant according to Eq. 7.

Both quantities have been introduced and discussed by Riekert (18) in the case of a similar triangular reaction network.

2.5.2. Potentiometric measurements. As stated above the oxygen activity a^2_{O} in the catalyst is operationally defined by the potentiometric measurement. Its value is related to the experimentally determined potential difference ΔE (open circuit potential) via the NERNST equation,

$$\Delta E = \frac{R \cdot T}{4 \cdot \text{F}} \cdot \ln \frac{a^2_{\text{O}}}{p_{\text{O}_2,\text{Ref}}}, \qquad [10]$$

where $p_{\text{O}_2,\text{Ref}}$ designates the oxygen partial pressure at the reference side and F is the FARADAY constant (F = 96, 486 C mol^{-1}). The relation is based on the potential-determining reaction R1, which takes place at the three-phase boundary line of gas–electrode–electrolyte at both electrodes.

$$\text{O}_{2,g} + 4e^-_{(\text{Electrode})} \leftrightarrow 2\text{O}^{2-}_{(\text{Electrolyte})}. \qquad [\text{R1}]$$

The oxygen activity in the solid is equal to the oxygen partial pressure in the gas phase if the oxygen in the gas phase is in equilibrium with the oxygen in the solid catalyst:

$$a^2_{\text{O}} \equiv p_{\text{O}_2}. \qquad [11]$$

This has been verified previously (15).

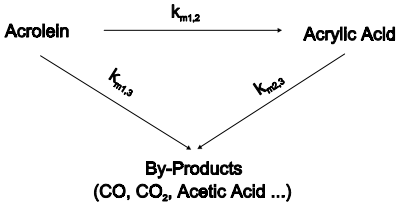

$$r_{\text{m}1,2} = \frac{k_{\text{m}1,2} \cdot c_{\text{Acrolein}}}{1 + b \cdot c_{\text{Acrolein}}} \qquad [4]$$

$$r_{\text{m}1,3} = \frac{k_{\text{m}1,3} \cdot c_{\text{Acrolein}}}{1 + b \cdot c_{\text{Acrolein}}} \qquad [5]$$

$$r_{\text{m}2,3} = k_{\text{m}2,3} \cdot c_{\text{Acrylic Acid}} \qquad [6]$$

FIG. 2. Network of acrolein oxidation and rate equations.

3. RESULTS

3.1. Results of the Kinetic Measurements

Typical results of the kinetic measurements over the single phases Mo–V–O_x and $CuMoO_4$ are shown in Fig. 3. The experimentally determined axial concentration profiles in the gas phase are plotted against the modified residence time t_m. The open symbols represent the measured concentration profiles over the copper molybdate, and the closed symbols over the Mo–V–O_x. The concentration profiles over the typical acrylic acid catalyst Mo–V–Cu–O_x and the mechanical mixture Mo–V–O_x/$CuMoO_4$ are not shown in this picture since they are quite similar to the profiles measured over the pure Mo–V–O_x. A detailed analysis of the reaction kinetics measured over Mo–V–Cu–O_x has been given in (12). The solid lines in Fig. 3 are the results of the model calculations using the values of the kinetic coefficients as obtained by the procedure described in the preceding paragraph. The agreement of the simulation with the experimental measurements justifies the description by the simplified network. The corresponding values of the kinetic coefficients and the derived characteristic parameters are given in Table 2.

Due to their high activity with respect to acrolein conversion the kinetic coefficients at 573 K for Mo–V–O_x, the mechanical mixture Mo–V–O_x/$CuMoO_4$, and the typical acrylic acid catalyst Mo–V–Cu–O_x are influenced by internal mass transport limitation. However, by variation of the shell thickness of the coated catalysts (we obtained the same values of $k_{mi,j}$ for catalysts with 5, 10, and 20 wt% active mass) we could show (15) that the influence of internal mass transfer is neglectable for all catalysts investigated at the lower temperature of 533 K.

Let us first discuss the results of the kinetic measurements obtained for the pure phases Mo–V–O_x and $CuMoO_4$.

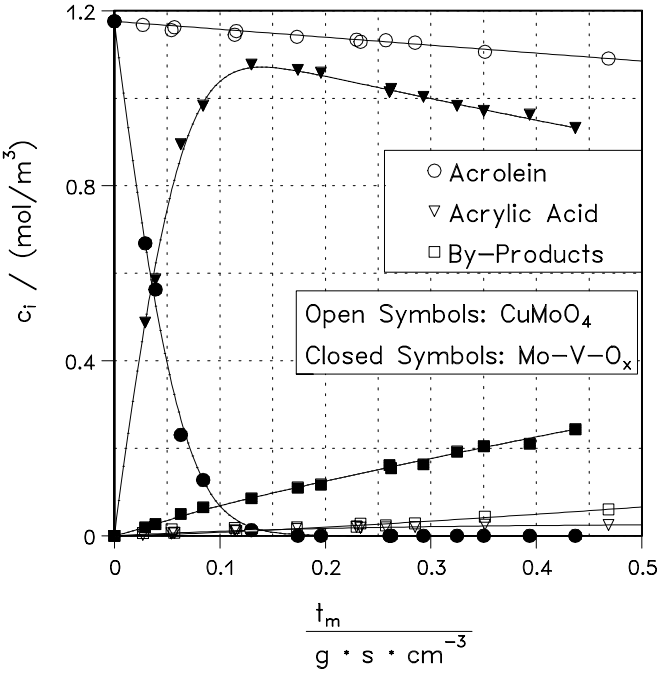

FIG. 3. Concentration profiles over $CuMoO_4$ and Mo–V–O_x during acrolein oxidation at 573 K, $y_{Acrolein,in} = 4$ vol%, $y_{O_2,in} = 11$ vol%, $y_{H_2O,in} = 5$ vol%.

The value of k^*_{m1} at 573 K for Mo–V–O_x is more than one order of magnitude higher than for $CuMoO_4$, indicating that Mo–V–O_x is the active phase in acrolein oxidation. The comparatively big value of the parameter b in the case of the copper molybdate shows that the concentration profiles over this phase could alternatively be described by using rate equations of zeroth order with respect to acrolein for the reaction pathways of acrolein consumption (cf. Fig. 2, reaction pathway 1,2 and 1,3). The zero-order rate

TABLE 2

Kinetic Coefficients and Characteristic Parameters of Acrolein Oxidation over $CuMoO_4$ (10 wt% of Active Mass), Mo–V–O_x, the Mechanical Mixture Mo–V–O_x/$CuMoO_4$, and the Typical Acrylic Acid Catalyst Mo–V–Cu–O_x

Catalyst	Kinetic parameters				Characteristic parameters			
	$^*k_{m1,2}$	$k_{m1,3}$	$k_{m2,3}$	b	$^K S_{Acrylic\ Acid}$	$^{int}\lambda_{Acrylic\ Acid}$	$Y^{max}_{Acrylic\ Acid}$	k^*_{m1}
$T = 533$ K								
$CuMoO_4$				Not determined				
Mo–V–O_x	21	1.14	0.13	2.1	0.95	111	0.92	15.2
Mo–V–O_x/$CuMoO_4$	28	0.6	0.08	7.1	0.98	138	0.95	11.3
Mo–V–Cu–O_x	23.3	0.3	0.16	3.2	0.99	86	0.95	14
$T = 573$ K								
$CuMoO_4$	1.9	0.8	4.6	16.3	$\cong 0.7$	0.09	<0.02	0.6
Mo–V–O_x	43	1.4	0.51	1.7	0.97	62	0.92	32.5
Mo–V–O_x/$CuMoO_4$	39	0.2	0.59	2.6	0.99	42	0.92	25.1
Mo–V–Cu–O_x	44	0	1	1.8	1	32	0.91	31.7

Note. All 20 wt% active mass; at 533 and 573 K, $y_{Acrolein,in} = 4$ vol%, $y_{O_2,in} = 11$ vol%, $y_{H_2O,in} = 5$ vol%.

constants describing the pathways of acrolein consumption could then be expressed by $(k_{m1,2}/b)$ and $(k_{m1,3}/b)$. It can be stated further that the acrolein conversion over $CuMoO_4$ was always below 10% even at a temperature of 573 K. Therefore, we did not determine the kinetic parameters at the lower temperature of 533 K in the case of the pure $CuMoO_4$. The low activity of $CuMoO_4$ with respect to acrolein conversion is equally illustrated by the low value of k^*_{m1}, which for the reason of comparison is computed for an acrolein conversion of 99% as before (although this conversion value could not be achieved with $CuMoO_4$ under the conditions stated).

In addition to the big difference concerning the activity with respect to acrolein conversion we can also observe a completely different selectivity behaviour between $CuMoO_4$ and Mo–V–O_x. In the case of Mo–V–O_x high values of the grain selectivity towards acrylic acid close to 1 were obtained. The grain selectivity is higher at 573 K (97%) than at 533 K (95%), indicating that the activation energy for reaction pathway 1,2 (acrolein to acrylic acid) is higher than for reaction pathway 1,3 (acrolein to by-products). Furthermore, the rate of oxidation of acrolein to acrylic acid is about two orders of magnitude higher than the rate of the consecutive oxidation of acrylic acid, as reflected by the high value of the stability parameter $^{int}\lambda$, which is one major reason for the high acrylic acid yield ($Y_{\text{Acrylic Acid}} = 92$ mol%) over Mo–V–O_x. In contrast to the grain selectivity the stability parameter of acrylic acid $^{int}\lambda$ decreases with increasing temperature, which can be explained by a higher activation energy for the reaction pathway 2,3 (acrylic acid to by-products) compared to the reaction pathway 1,2 (acrolein to acrylic acid).

In the case of pure $CuMoO_4$ the values of acrylic acid selectivity have to be considered with caution (cf. Fig. 4). One has to keep in mind that the selectivity of acrylic acid formation is calculated as the ratio of the observed values of acrylic acid yield and acrolein conversion. As a consequence the values of acrylic acid selectivity might scatter at low values of acrolein conversion ($X < 3\%$), as obtained with $CuMoO_4$. In this region of acrolein conversion ($X < 3\%$) the error in acrylic acid selectivity is of an order that a reasonable confidence interval cannot be given. Nevertheless, we can say that the main reason for the low acrylic acid yield over $CuMoO_4$ is the fact that the selectivity towards acrylic acid sharply decreases with increasing acrolein conversion, as shown by the decrease in acrylic acid selectivity and the curvature of the line for acrolein conversion, >3%. For a conversion of about 10% the selectivity towards acrylic acid only amounts to 20%, although the grain selectivity seems to be in the range of 70%. Thus, it is obvious that acrylic acid, once formed over $CuMoO_4$, is immediately subject to overoxidation to by-products. This is also reflected by the comparatively high value of $k_{m2,3}$, indicating a high rate of the consecutive reaction over $CuMoO_4$ (cf. Table 2). As a consequence of the low reaction rate of

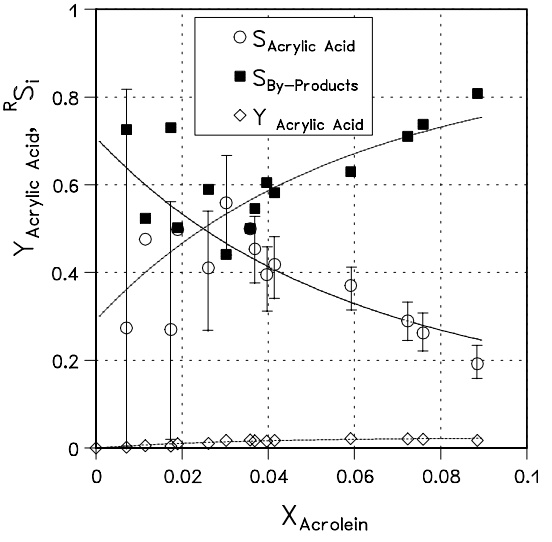

FIG. 4. Reactor selectivity and yield with respect to acrylic acid as a function of acrolein conversion over $CuMoO_4$ at 573 K, $y_{\text{Acrolein,in}} =$ 4 vol%, $y_{O_2,\text{in}} = 11$ vol%, $y_{H_2O,\text{in}} = 5$ vol%.

acrolein oxidation to acrylic acid on the one hand and the high reaction rate of acylic acid oxidation to by-products on the other hand, the value of $^{int}\lambda$ is far below 1 in the case of $CuMoO_4$ (cf. Table 2).

Let us now consider the kinetic behaviour of the mechanical mixture $CuMoO_4$/Mo–V–O_x and the typical acrylic acid catalyst Mo–V–Cu–O_x (cf. Fig. 5).

Generally we can say that the kinetics of acrolein oxidation are similar over the pure Mo–V–O_x, the mechanical mixture $CuMoO_4$/Mo–V–O_x, and the typical acrylic

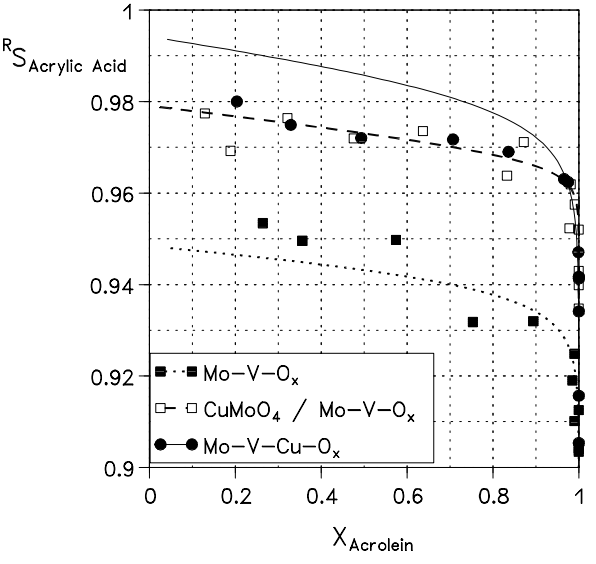

FIG. 5. Reactor selectivity with respect to acrylic acid as a function of acrolein conversion over Mo–V–O_x, the mechanical mixture Mo–V–O_x/$CuMoO_4$, and the typical acrylic acid catalyst Mo–V–Cu–O_x at 533 K, $y_{\text{Acrolein,in}} = 4$ vol%, $y_{O_2,\text{in}} = 11$ vol%, $y_{H_2O,\text{in}} = 5$ vol%.

acid catalyst Mo–V–Cu–O_x. The mass-related activity of the mechanical mixture and the typical acrylic acid catalyst with respect to acrolein conversion is slightly lower than for pure Mo–V–O_x (cf. value of k^*_{m1} in Table 2). However, the most striking difference between pure Mo–V–O_x on the one hand and the mechanical mixture $CuMoO_4$/Mo–V–O_x and the typical acrylic acid catalyst Mo–V–Cu–O_x on the other hand concerns their selectivity behaviour. At an acrolein conversion below 95% the acrylic acid selectivity is always higher in the case of the mechanical mixture and the typical acrylic acid catalyst at both temperatures investigated (cf. Fig. 5). This is mainly due to the higher grain selectivity towards acrylic acid observed for the mechanical mixture and Mo–V–Cu–O_x (cf. Table 2). As a consequence of the higher grain selectivity we could increase the maximum yield of acrylic acid at 533 K from 92 to 95% by adding $CuMoO_4$ to Mo–V–O_x. However, at 573 K the maximum yield of acrylic acid is about the same as for the pure Mo–V–O_x, the mechanical mixture $CuMoO_4$/Mo–V–O_x, and the typical acrylic acid catalyst Mo–V–Cu–O_x, although the grain selectivity towards acrylic acid stays significantly higher in the case of the mechanical mixture (99 compared to 97%) and Mo–V–Cu–O_x (100 compared to 97%). The reason is illustrated by the lower value of the stability parameter $^{int}\lambda$ obtained for both the mechanical mixture and Mo–V–Cu–O_x (cf. Table 2), which seems to point out that the addition of $CuMoO_4$ to Mo–V–O_x enhances the rate of overoxidation of acrylic acid to by-products, as is also indicated by the kinetic measurements over the pure $CuMoO_4$. This effect seems to become more pronounced for the high temperature of 573 K. Both effects, the increase in the grain selectivity to acrylic acid on one hand and the decrease in the stability of acrylic acid on the other hand, compensate for each other with respect to the maximum acrylic acid yield at 573 K.

3.2. *Results of the Potentiometric Measurements*

Let us now consider the evolution of the oxygen activity in the separate phases Mo–V–O_x and $CuMoO_4$ as a function of the concentration profiles along the fixed-bed reactor (cf. Fig. 6). As explained in Section 2 all potentiometric measurements have been performed using the same catalyst in the fixed-bed reactor (Mo–V–Cu–O_x, 10 wt% active mass). Thus the resulting concentration profiles, represented by the closed symbols in Fig. 6, remain the same.

A continuous profile for the oxygen activity was obtained for both phases. The values of the oxygen activity are always at least 11 orders of magnitude lower than the oxygen partial pressure of the corresponding gas phase over the catalyst. This clearly indicates a partially reduced state of both catalysts rather than an equilibrium between the oxygen in the catalyst and in the surrounding gas phase. In the latter case the oxygen activity should be equal to the oxygen partial pressure (cf. Eq. 11).

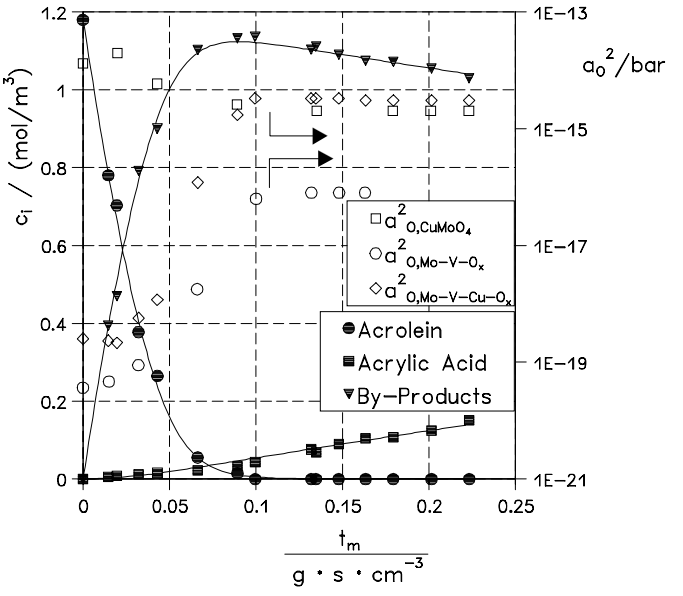

FIG. 6. Concentration profiles (left axis) and oxygen activity profiles (right axis) as a function of the modified residence time over $CuMoO_4$, Mo–V–O_x, and Mo–V–Cu–O_x at 573 K, $y_{Acrolein,in} = 4$ vol%, $y_{O_2,in} = 11$ vol%, $y_{H_2O,in} = 5$ vol%.

The oxygen activity profile for Mo–V–O_x is quite similar to that obtained for the typical acrylic acid catalyst Mo–V–Cu–O_x, which has been discussed in detail in (12) and is also shown in Fig. 6 for a better understanding. Over the whole range the values of the oxygen activity of Mo–V–O_x are about one order of magnitude lower than the values obtained for Mo–V–Cu–O_x.

From the reactor entrance on, the values of a_O^2 for Mo–V–Cu–O_x and Mo–V–O_x remain at a low level over a wide range of acrolein conversion ($X = 75\%$). This is surprising since the molar fraction of acrolein decreases from 4% at reactor inlet to 1%. If the acrolein conversion is near 100%, the oxygen activity strongly increases, reaching a constant level at complete acrolein conversion, where acrolein is no longer detectable in the gas phase by gas chromatography.

A completely different oxygen activity profile was observed in the case of the pure $CuMoO_4$ (open squares in Fig. 6). First of all we can say that the values for the oxygen activity of $CuMoO_4$ in contact with the reaction mixture at the reactor entrance are about five orders of magnitude higher than in the case of Mo–V–O_x and Mo–V–Cu–O_x. Furthermore we obtain a lower value of the oxygen activity if $CuMoO_4$ is in contact with the reaction mixture at the reactor outlet (complete acrolein conversion) than if it is in contact with the reaction mixture at the reactor inlet. This indicates that in the case of the pure $CuMoO_4$ acrylic acid is a stronger reducing agent than acrolein. The removal of oxygen from $CuMoO_4$ by oxidation of acrylic acid to CO and CO_2 takes place at a higher rate than by the oxidation of acrolein. This important result is totally in agreement

with the results obtained from the kinetic measurements. The value of $^{int}\lambda$, which is below 1 in the case of the pure $CuMoO_4$, shows that the rate coefficient of acrylic acid oxidation is higher than the rate coefficient of acrylic acid production by acrolein oxidation.

The situation in the case of Mo–V–O_x and Mo–V–Cu–O_x is just the opposite. For both catalysts the oxygen activity at the reactor entrance is lower than for complete acrolein conversion and accordingly the values of $^{int}\lambda$ (cf. Table 2) are clearly above 1.

4. DISCUSSION

In the present study of selective oxidation of acrolein the gas-phase composition and the oxidation state of different oxidic catalysts, represented by their oxygen activity, were both monitored by simultaneous kinetic and potentiometric measurements. Both measurements led to consistent results.

The results of the kinetic measurements show that Mo–V–O_x is the active and selective phase during acrolein oxidation, whereas $CuMoO_4$ alone is more or less inactive and unselective with respect to acrolein oxidation. At this point the question arises as to whether synergistic effects concerning the kinetics can be observed in a mixture of both phases. Therefore, we also determined the kinetics of acrolein oxidation over the mechanical mixture Mo–V–O_x/$CuMoO_4$ and over the typical acrylic acid catalyst Mo–V–Cu–O_x.

Let us first consider the activity with respect to the consumption of acrolein, which is characterised by the kinetic parameter k^*_{m1}. In a plot of k^*_{m1} over the $CuMoO_4$ content in the active mass of the catalysts, the values of k^*_{m1} for all catalysts which do not show synergetic effects are given by the straight line fixed by the values for the pure phases Mo–V–O_x and $CuMoO_4$ (cf. Fig. 7). If the value of k^*_{m1} lies above this line we speak of a synergetic effect. As we can see in Fig. 7 the values of k^*_{m1} at both the mechanical mixture and the typical acrylic acid catalyst differ only by less than 15% from the linear relationship. Thus, concerning the activity of acrolein conversion $CuMoO_4$ acts as a diluent when mixed with Mo–V–O_x and we cannot speak of a synergetic effect.

In contrast to activity a remarkable synergetic effect could be observed concerning the selectivity of acrolein consumption. The addition of $CuMoO_4$ to Mo–V–O_x significantly increases the grain selectivity towards acrylic acid (cf. Table 2 and Fig. 5) at both temperatures investigated (533 and 573 K). As a consequence the maximum acrylic acid yield at 533 K was higher with the mixed catalysts (Mo–V–O_x/$CuMoO_4$ and Mo–V–Cu–O_x) than with the pure Mo–V–O_x. However, at the higher temperature of 573 K the addition of $CuMoO_4$ to Mo–V–O_x leads to more overoxidation of acrylic acid, thus decreasing the stability parameter of acrylic acid $^{int}\lambda$, as also reflected by the kinetic results obtained for the pure $CuMoO_4$, for which the rate of acrylic acid oxidation is much higher than the rate of acrolein oxidation (cf. Fig. 4). Therefore, the maximum acrylic acid yield at 573 K was the same for the pure Mo–V–O_x and the mixed catalysts. Due to the described phenomena the maximum acrylic acid yield at temperatures above 573 K should be higher for the pure Mo–V–O_x than for the mixed catalysts. The negative influence of $CuMoO_4$ with respect to the total oxidation of acrylic acid at the high temperature of 573 K might be due to an aggregation of $CuMoO_4$ clusters serving as centres of total oxidation.

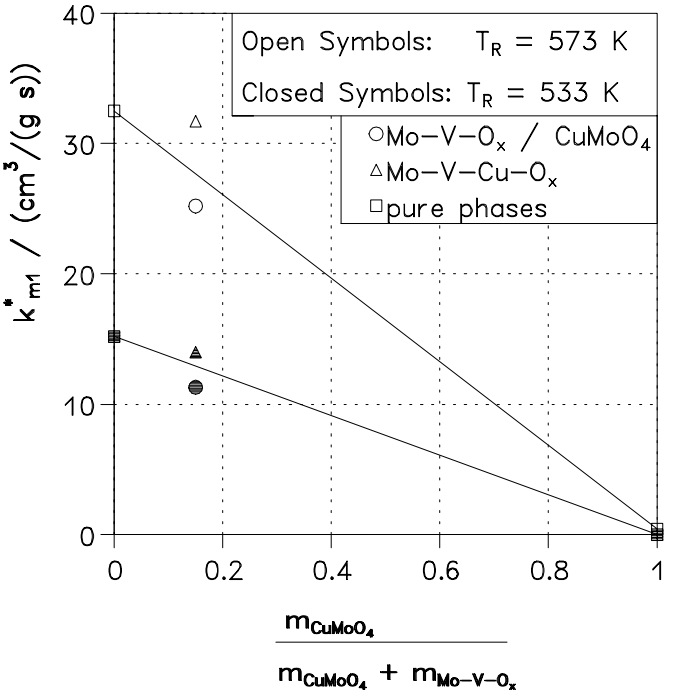

FIG. 7. k^*_{m1} as a function of the $CuMoO_4$ content; $y_{Acrolein,in}$ = 4 vol%, $y_{O_2,in}$ = 11 vol%, $y_{H_2O,in}$ = 5 vol%.

From these results we would expect the maximum acrylic acid yield for an isothermal operated reactor at 573 K over a structured catalyst bed containing the mixture Mo–V–O_x/$CuMoO_4$ in the first zone and pure Mo–V–O_x in the second.

The described results are especially important for the operation of a commercial acrylic acid reactor since even a small gain of acrylic acid yield leads to a remarkable cost reduction of the production process.

The results of the potentiometric measurement are consistent with the results obtained from the kinetic measurements. In the case of the pure $CuMoO_4$ the potentiometric measurements indicate that the removal of oxygen from $CuMoO_4$ by oxidation of acrylic acid to CO and CO_2 takes place at a higher rate than by the oxidation of acrolein. This is totally in agreement with the low value of the stability parameter ($^{int}\lambda < 1$) observed for $CuMoO_4$, which shows that the rate coefficient of acrylic acid oxidation is higher than the rate coefficient of acrylic acid production by acrolein

oxidation. In this sense we could think of applying SEP to test oxidic phases with respect to the stability of the desired intermediate of a selective oxidation reaction over these phases. The oxygen activity of the oxidic catalyst in contact with a gas phase containing the intermediate (here: acrylic acid) should always be higher than in contact with a gas phase containing the starting material (here: acrolein) to obtain a reasonable stability of the intermediate.

Furthermore, the potentiometric measurements might point out the reason for the synergetic effect in the case of acrolein oxidation over Mo–V–Cu–O_x: The results of the potentiometric measurements show that under the same reaction conditions the oxygen activity in the pure $CuMoO_4$ is always higher than in the pure Mo–V–O_x. Let us now consider a mixture of both phases in which $CuMoO_4$ and Mo–V–O_x exist side by side without forming a new oxidic phase. In this case $CuMoO_4$ could principally serve as an oxygen donor and the Mo–V–O_x as an oxygen acceptor when exposed to a gas phase which contains acrolein and oxygen. Oxygen is transferred from $CuMoO_4$ to Mo–V–O_x driven by the gradient in the oxygen activity. The oxygen transfer between the solids can generally proceed via the bulk and via the catalyst surface, the latter being called spillover. The application of SEP does not allow discrimination between both transfer mechanisms. However, the oxygen transfer from $CuMoO_4$ to Mo–V–O_x results in an oxygen activity characterising the mixture of both phases, which lies between the values of the oxygen activity of the pure phases. Although the typical acrylic acid catalyst Mo–V–Cu–O_x is prepared in a one-pot synthesis it can be regarded as a mixture of mainly Mo–V–O_x and $CuMoO_4$. Due to the one-pot synthesis both phases should be highly dispersed, which indicates that oxygen transfer between $CuMoO_4$ and Mo–V–O_x can take place quite effectively in Mo–V–Cu–O_x, leading to a homogenous oxygen activity over the whole solid. Indeed, the oxygen activity in Mo–V–Cu–O_x lies between the values for the pure phases $CuMoO_4$ and Mo–V–O_x (cf. Fig. 6), indicating the direction of oxygen transfer in Mo–V–Cu–O_x from $CuMoO_4$ to Mo–V–O_x (cf. Fig. 8).

It has been shown recently (19) that the redox model proposed by Mars and van Krevelen (20) can be applied to the acrolein oxidation over Mo–V–Cu–O_x. In accordance with that model Andrushkevich *et al.* (10) observed that strongly bound lattice oxygen is used preferentially in the selective oxidation of acrolein to acrylic acid whereas the unselective side reaction to by-products is due to weakly bound adsorbed oxygen species. Keeping this in mind we may assume that the oxygen species transferred in Mo–V–Cu–O_x are mainly incorporated in the lattice to reoxidize reduced active sites of Mo–V–O_x. Thus the oxygen transferred from $CuMoO_4$ to Mo–V–O_x should always act selectively, forming acrylic acid, and the addition of $CuMoO_4$ to Mo–V–O_x leads to an increased selectivity, as observed in both the industrially used Mo–V–Cu–O_x and the mechanical mixture Mo–V–O_x/$CuMoO_4$.

Other explanations for the observed phase synergism cannot be ruled out. For example, applying the concept of "site isolation" we may assume that $CuMoO_4$ partly covers Mo–V–O_x and therefore limits the amount of available oxygen at an active site of Mo–V–O_x. As a consequence the rate of the total oxidation reaction of acrolein to CO and CO_2 would be suppressed.

However, SEP gives a strong hint that oxygen is transferred from $CuMoO_4$ to Mo–V–O_x independently of its function in the catalytic cycle.

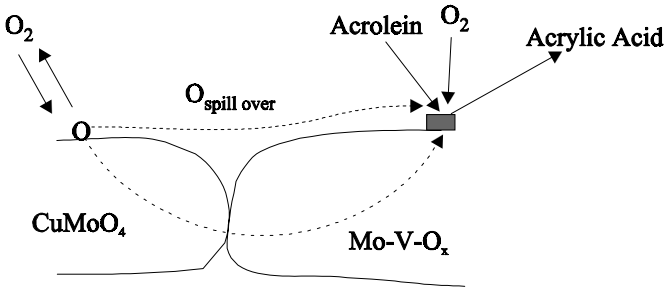

FIG. 8. Schematic drawing of the oxygen transfer in Mo–V–Cu–O_x.

ACKNOWLEDGMENT

The present work has been sponsored by the Ministry of Research and Technology of the German Federal Republic through Contract 03 D 0006.

REFERENCES

1. Krabetz, R., *et al.*, European Patent 17,000 (1980).
2. Recknagel, R., and Riekert, L., *Chem. Tech.* **46**, 324 (1994).
3. Haber, J., *Stud. Surf. Sci. Catal.* **72**, 279 (1992).
4. Callahan, J. L., and Grasselli, R. K., *AIChE J.* **9**, 755 (1963).
5. Delmon, B., and Weng, L. T., *Appl. Catal. A* **81**, 141 (1992).
6. Teichner, S. J., *Stud. Surf. Sci. Catal.* **77**, 27 (1993).
7. Moro-Oka, Y., *Stud. Surf. Sci. Catal.* **77**, 95 (1993).
8. Ozkan, U., Moctezuma, E., and Driscoll, S. A., *Appl. Catal.* **58**, 305 (1990).
9. Weismantel, L., and Emig, G., *Chem.-Ing.-Tech.* **68**, 721 (1996).
10. Andrushkevich, T. V., *Catal. Rev.–Sci. Eng.* **35**(2), 213 (1993).
11. Wagner, C., *Adv. Catal.* **21**, 323 (1970).
12. Estenfelder, M., and Lintz, H.-G., *J. Catal.* **195**, 38 (2000).
13. Wiesmann, M., Ehrenberg, H., Miehe, G., Penn, T., Weitzel, H., and Fuess, H., *J. Solid State Chem.* **132**, 88 (1997).
14. Werner, H., Timpe, O., Herein, D., Uchida, Y., Pfänder, N., Wild, U., and Schlögl, R., *Catal. Lett.* **44**, 153 (1997).
15. Estenfelder, M., Thesis. University of Karlsruhe (TH), Karlsruhe, Germany, 1998.
16. Recknagel, R., Thesis. University of Karlsruhe (TH), Karlsruhe, Germany, 1994.
17. Breiter, S., and Lintz, H.-G., *Chem. Eng. Sci.* **50**, 785 (1995).
18. Riekert, L., *Appl. Catal.* **15**, 89 (1985).
19. Estenfelder, M., Lintz, H.-G., Stein, B., and Gaube, J., *Chem. Eng. Process.* **37**, 109 (1998).
20. Mars, P., and van Krevelen, D. W., *Spec. Suppl. Chem. Eng. Sci.* **3**, 41 (1954).